Published in final edited form as:
J Am Chem Soc. 2009 November 11; 131(44): 16119–16126. doi:10.1021/ja904072s.

Gramicidin Pores Report the Activity of Membrane-Active Enzymes

Sheereen Majd[†], **Erik C. Yusko**[†], **Alexander D. MacBriar**[†], **Jerry Yang**[‡,*], and **Michael Mayer**[†,*]

[†] Department of Chemical Engineering and Department of Biomedical Engineering, University of Michigan, 1101 Beal Avenue, Ann Arbor, Michigan 48109-2110

[‡] Department of Chemistry and Biochemistry, University of California, San Diego, 9500 Gilman Drive, MC 0358, La Jolla, California 92093-0358

Abstract

Phospholipases constitute a ubiquitous class of membrane-active enzymes that play a key role in cellular signaling, proliferation, and membrane trafficking. Aberrant phospholipase activity is implicated in a range of diseases including cancer, inflammation, and myocardial disease. Characterization of these enzymes is therefore important, both for improving the understanding of phospholipase catalysis, and for accelerating pharmaceutical and biotechnological applications. This paper describes a novel approach to monitor, *in-situ* and in real-time, the activity of phospholipase D (PLD) and phospholipase C (PLC) on planar lipid bilayers. This method is based on enzyme-induced changes in the electrical charge of lipid bilayers and on the concomitant change in ion concentration near lipid membranes. The approach reports these changes in local ion concentration by a measurable change in the ion conductance through pores of the ion channel-forming peptide gramicidin A. This enzyme assay hence takes advantage of the amplification characteristics of gramicidin pores to sense the activity of picomolar to nanomolar concentrations of membrane-active enzymes without requiring labeling of substrates or products. The resulting method proceeds on lipid bilayers without the need for detergents, quantifies enzyme activity on native lipid substrates within minutes, and provides unique access to both leaflets of well-defined lipid bilayers; this method also makes it possible to generate planar lipid bilayers with transverse lipid asymmetry.

Introduction

Phospholipases are membrane-active enzymes that catalyze the hydrolysis of specific ester bonds in phospholipids. These enzymes play a critical role in cell signaling, proliferation, and vesicle trafficking.[1–3] As a result, phospholipases are implicated in a range of diseases including cancer, inflammation, and myocardial disease.[1–3] To improve the understanding of these enzymes, characterization methods that monitor the activity of phospholipases *in situ*, in real time, and in a label-free fashion, would be useful. Due to the heterogeneous nature of catalytic reactions on lipid membranes it is, however, often challenging to monitor the activity of membrane-active enzymes.[4,5] Established methods to characterize phospholipases measure the absorbance, fluorescence, or radioactivity of their enzymatic products.[3,5,6] While

Michael Mayer, Department of Chemical Engineering and Department of Biomedical Engineering, University of Michigan, 1101 Beal Avenue, Ann Arbor, MI 48109-2110. Phone: (734) 763-4609, Fax: (734) 647-4834, mimayer@umich.edu., Jerry Yang, Department of Chemistry and Biochemistry, University of California, San Diego 9500 Gilman Drive, MC 0358, La Jolla, CA 92093. Phone: (858) 534-6006, Fax: (858) 534-4554, jerryyang@ucsd.edu.

Supporting Information Available. Additional information and experimental details. This information is available free of charge via the Internet at http://pubs.acs.org/.

radioactive and fluorescent assays offer high sensitivity, these assays are often not performed *in situ*, and the need for labeling of the substrate can limit the application or affect the results of these assays. Other assays employ coupled enzyme reactions[1,7,8] in which the optimum experimental condition may be limited by the second enzyme. More recently, liquid crystals were employed for label-free detection of phospholipase activity, however, this approach is not quantitative.[9]

Here, we describe a novel, label-free, rapid, and quantitative method to monitor, *in situ*, the activity of phospholipases D and C (PLD, PLC) on planar lipid bilayers. This approach offers high sensitivity by ion channel amplification[10,11] and employs planar lipid bilayers instead of micelles or liposomes. The assay hence provides access to both leaflets of a bilayer—a unique characteristic that makes this assay platform attractive for generating asymmetric lipid bilayers by adding different enzymes to each side of a membrane.

PLD cleaves the phosphodiester bond on the polar side of phospholipid headgroups (Fig. 1a) while PLC cleaves the bond on the glycerol side (Fig. 1b).[1,3,5] These phospholipases, therefore, modify the headgroup of phospholipids and, for many lipid substrates, this modification results in a change in the net charge of the lipid molecule. In solutions of low ionic strength (i.e. close to, or below the physiologic range) this enzyme-induced change in the electric charge on the lipids in a membrane results in a change of the local concentration of counter ions near the membrane surface.[12] This change in ion concentration can be detected by the channel-forming peptide gramicidin A (gA).[11,13,14] Hence, the enzyme assays introduced here, take advantage of the change in the single-channel ion conductance through gA pores, γ, in response to enzyme-catalyzed modifications of the charge of lipids.[11,14] Fig. 2 illustrates this concept for PLD.

Results and Discussion

Monitoring the Enzymatic Activity of PLD

In order to demonstrate the ability of an assay based on gA to monitor the activity of PLD, we formed planar lipid bilayers containing phosphatidylcholine (PC) lipids as substrate and monitored the changes in single channel conductance of gA, γ, upon addition of PLD from cabbage (EC 3.1.4.4) to both sides of the bilayer.[17] After addition of the enzyme to the bilayer, we recorded short ($\leq$ 60 s) current traces at different applied voltages and at distinct points of time after enzyme addition (Fig. 3). To analyze these current versus time traces, we first obtained a histogram that represented the distribution of currents for each current trace (Fig. 3). The difference in current between adjacent peaks in these histograms represented the current amplitude of single gA channel openings. These current amplitudes, therefore, reflect the single channel conductance of gA, γ, at a given time after addition of PLD. By averaging all current amplitudes within a histogram, we obtained the mean current amplitude of gA events and a standard deviation (SD) for these mean current amplitudes for each trace that corresponded to a certain time after addition of the enzyme. We plotted these mean current amplitudes with their SDs as a function of the applied voltage for each time point. From these I–V plots, we obtained a mean value for single channel conductance of gA, γ, at a given time point from the slope in the linear range $\leq |\pm 100$ mV| of the plot according to the equation $I = R^{-1} \cdot V = \gamma \cdot V$.

As demonstrated in Fig. 3, the current amplitude of gA opening and closing events increased over time after addition of PLD to the bilayer setup. To further illustrate the shift in the amplitude of single channel currents upon addition of PLD, we plotted the distribution of the step amplitudes as a consequence of each opening and closing event in the original current versus time traces in Fig. 4. These event histograms clearly illustrate the time-dependent increase in step amplitude of gA events after addition of PLD.

Given the reaction equation of PLD (Fig. 1a), we hypothesized that this increase in current amplitude of gA events was due to the formation of the negatively-charged PA lipids (the product of PLD-catalyzed hydrolysis of neutral PC lipids) in the bilayer. In order to test this hypothesis, we measured the current amplitude of gA events in membranes of various PA contents. Fig. 5a and b show the statistical distribution of the current amplitude of gA events in PC bilayers as a function of the mole fraction of PA in the bilayer. As expected, these results illustrated a significant increase in the mean current amplitude of gA events as a result of increasing amounts of PA lipids in the bilayer.

In order to relate, quantitatively, the changes in γ to the changes in amount of produced PA lipids in the membrane, we acquired a calibration curve (Fig. 5c) of γ (in units of pS = 10^{-12} Ω^{-1}) as a function of the mole fraction of phosphatidic acid (X_{PA}, unitless). Eq. 1, which resulted from the curve fit in Fig. 5c, describes this calibration curve:[18]

$$\gamma = \frac{3.50\ \text{pS} + (12.83\ \text{pS} \times X_{PA})}{(0.23 + X_{PA})}. \quad (1)$$

Fig. 6 demonstrates the time-dependent increase in γ after addition of different amounts of PLD to a PC bilayer. Interestingly, this increase progressed with an initial lag phase of slow change, followed by a rapid increase in γ. We considered two possible effects to explain this lag phase (which lasted 5–9 min depending on the enzyme concentration). First, Kuppe et *al.* have previously reported a similar lag phase of slow activity of PLD on PC bilayers.[8] These authors demonstrated that Ca^{+}-induced formation of PA domains in PC membranes[19] is a key parameter that facilitates binding of PLD to the membrane surface and significantly increases the hydrolysis rate of PLD.[8] Second, mixing of PLD in the electrolyte of the bilayer chamber and binding of PLD to PC membranes may take time.

To estimate the change in X_{PA} in membranes upon addition of PLD, we used Eq. 1. Fig. 7a shows the linear, time-dependent changes in X_{PA} after the lag phase for different PLD concentrations. We defined the lag time as the interval from addition of PLD until X_{PA} reached a value of ~0.03 (see Supporting Information for details). The inset in Fig. 7a reveals that the rate of product formation (dX_{PA}/dt) increased linearly with an increase in enzyme concentration.

To confirm a functional dependence of γ on the enzymatic activity of PLD, we performed a control experiment with heat-denatured PLD and found no increase in γ (Fig. 7b). Furthermore we monitored the changes in γ upon addition of PLD in the presence of two PLD inhibitors, resveratrol[3,20] and cyclosporine A.[21] Fig. 7b shows that both inhibitors reduced the reaction rate significantly. We also examined the effect of the soluble product of the reaction, choline, on γ and found no significant change in the presence of 20 μM choline (see Supporting Information).

In addition, we examined the effect of the lipid product of the reaction, PA, on the permeability of ions through the bilayer[19] in the absence of gA pores and found no significant effect in the examined range of 0–30 mol% PA content (see Supporting information).

Together, these control experiments confirmed that the increase in γ upon addition of PLD was due to enzymatic activity and not due to artifacts.

Generating Asymmetric Bilayers by Enzymatic Activity of PLD

To explore the potential of this gA-based assay platform to create asymmetric planar lipid bilayers, we exposed one side of a PC bilayer to active PLD and the other side to inactivated PLD (Fig. 8a). We hypothesized that asymmetric activity of the enzyme would create a planar bilayer with transverse asymmetry, in which one leaflet (exposed to active PLD) would contain the catalytic product, i.e. negatively-charged PA lipids, and the other leaflet (exposed to inactivated PLD) would retain unmodified substrate, i.e. neutral PC lipids. We have previously demonstrated that γ is affected only by the electric charges present near the *entrance* of gA channels and not by the charges near the *exit* of the pore.[11] Since gA is permeable to cations, the entrance of gA pores is always located in the positively polarized compartment of the bilayer setup. Hence, the entrance of gA channels can be switched from one compartment to the other based on the polarity of applied voltage. We, therefore, hypothesized that if asymmetric activity of PLD on the PC bilayer produces a bilayer with transverse lipid asymmetry, gA pores would have a large conductance when the polarity of the voltage would place the entrance of gA on the side of the negatively-charged leaflet (i.e., the side with active PLD), whereas gA pores would have a low conductance when the polarity of the voltage would place the entrance on the side of the neutral leaflet of the bilayer (i.e., the side with inactive PLD).

Fig. 8b shows that, as expected, γ changed asymmetrically depending on the polarity of the applied voltage: at +100 mV, γ increased strongly over time (with this polarity, the entrance of the gA pores was located on the side with active PLD), whereas γ did not increase significantly at −100 mV, when the polarity placed the gA entrance on the side with inactive PLD.

To describe the relationship between γ and the time after addition of PLD, we derived an equation to fit the data in Fig. 8b. As shown by Eq. 1, γ is a hyperbolic function of the mole fraction of PA in the membrane, X_{PA}, while we used a simple model to describe the relationship between X_{PA} and time, t, after addition of PLD by a rate equation for pseudo-first order kinetics of the form:[22]

$$X_{PA}=1-e^{-kt}, \tag{2}$$

where the fitting parameter k (min^{-1}) is a pseudo-first order rate constant of the overall reaction at a given concentration of PLD. Combining Eq. 1 and Eq. 2, we obtained the functional dependence of γ on the time t after addition of PLD:

$$\gamma=3.50\ \text{pS}+\frac{12.83\ \text{pS}\times(1-e^{-k(t-t_0)})}{0.23+(1-e^{-k(t-t_0)})}. \tag{3}$$

We introduced t_0 (min) in Eq. 3 to account for the lag phase. The solid red curve in Fig. 8b illustrates the best fit of the six points shown in red after the lag phase to Eq. 3, with k = 0.02 min^{-1} and t_0 = 3.16 min for the best fit.

The strong difference between γ as a function of the polarity of the applied voltage in Fig. 8b demonstrates the ability of the platform presented here to create asymmetric lipid bilayers by asymmetric addition of an enzyme to a symmetric planar bilayer. Although not demonstrated in this paper, we think that this capability is attractive since intracellular lipases process lipids in natural biomembranes with strong transverse asymmetry. The assay developed here, may hence make it possible to study lipase activity in bilayers that are better models of physiologic membranes than liposomes or micelles. In addition, the capability of generating asymmetric

lipid bilayers by exploiting lipase activity as demonstrated here, may be useful for studying the effect of transverse asymmetry on the activity of other membrane proteins, such as ion channels and transport proteins. And finally, the results from asymmetric addition of enzymes shown in Fig. 8, provide additional evidence that the observed changes in γ were indeed due to the enzyme activity of phospholipase and not due to artifacts.

Monitoring the Enzymatic Activity of PLC

In order to extend this label-free, ion channel-based approach of quantifying enzyme activity to a second relevant enzyme, we monitored the activity of phosphatidylinositol-specific PLC (PI-PLC) from *Bacillus cereus* (EC 3.1.4.10). In this case, we recorded the changes in γ in PC bilayers that contained initially 10 % PI (i.e. $X_{PI,0} = 0.1$) upon addition of the PI-PLC enzyme.

In these experiments, as PI-PLC catalyzed the hydrolysis of negatively-charged PI lipids and produced neutral diacylglycerol (DAG) lipids[15] (Fig. 1b), the concentration of cations close to the membrane surface gradually decreased, leading to a measurable reduction of γ. Fig. 9a shows a calibration curve of γ as a function of X_{PI}. Eq. 4, which resulted from the curve fit in Fig. 9a, describes this calibration curve:

$$\gamma = \frac{8.65\ \text{pS} + (8.26\ \text{pS} \times X_{PI})}{(0.07 + X_{PI})}. \quad (4)$$

Based on the measured values of γ we used Eq. 4, to estimate X_{PI} as a function of time after addition of PI-PLC. Fig. 9b shows the decrease in X_{PI} after addition of ~40 and ~80 pM of PI-PLC. The initial slopes of the two resulting exponential fits in Fig. 9a, differed by a factor of 2.1 and were hence close to the expected value of 2.0.

Limit of Detection of gA-Based Assays of Membrane-Active Enzymes

The limit of detection (LOD) of these assays (based on LOD = 3 × standard deviation) was equal to a mole fraction of PA, X_{PA}, of 0.003 for the PLD assay, and a mole fraction of PI, X_{PI}, of 0.078 for the PLC assay (see Supporting Information for details). We obtained these limits of detection with an ionic strength of ~21.5 mM; the sensitivity of the assay decreases with increasing ionic strength because the effect of electrostatic attraction of cations near a negatively-charged membrane surface will contribute relatively less to γ than the increased concentration of cations in the bulk solution.[11,14] Nevertheless, we and others showed previously that negatively-charged membranes still increase γ significantly at ionic strengths close to the physiologic range (e.g. at 100 mM KCl).[11,14]

Conclusion

In summary, this work presents a novel, label-free assay to monitor, in real time, the enzymatic activity of phospholipases D and C on planar lipid bilayers. This ion channel-based assay provides unique access to both leaflets of a bilayer, proceeds on membranes with well-defined lipid composition, and exploits amplification characteristics of an ion pore[11] (see Supporting Information). In addition, this assay detects enzyme activity within minutes at picomolar to nanomolar concentrations of membrane-active enzymes on native lipid substrates without requiring detergents or labels. Finally, this assay platform makes it possible to generate planar lipid bilayers with transverse lipid asymmetry. The application of the present ion channel-based assay may be somewhat limited by the poor mechanical stability of planar lipid bilayers. Recently reported strategies for fabrication of mechanically-stable bilayers[23–25] such as embedding lipid bilayers in hydrogels[26] may, however, address this issue in future work.

Experimental Section

Materials

We purchased cesium acetate, resveratrol, and cyclosporin A from Sigma Aldrich; potassium chloride (KCl) from EMD Chemicals; cesium chloride (CsCl) from International Biotechnologies, Inc.; calcium chloride ($CaCl_2$), pentane, and hexadecane from Fluka; and HEPES from Fisher Scientific. Gramicidin A (gA) was purchased as gramicidin D from Sigma Aldrich and purified by silica chromatography as described previously[27] to afford a final purity of 97% of gA. We purchased the following phospholipids form Avanti Polar Lipids, Inc.: 1,2-diphytanoyl-*sn*-glycero-3-phosphocholine (DiPhyPC), 1,2-diphytanoyl-*sn*-glycero-3-phosphate (sodium salt) (DiPhyPA), and 1,2-dioleoyl-*sn*-glycero-3-phosphoinositol (ammonium salt) (PI). Phospholipase D (PLD) from cabbage (EC 3.1.4.4) was obtained from Sigma Aldrich and phosphatidylinositol-specific phospholipase C (PI-PLC) from *Bacillus cereus* (EC 3.1.4.10) was purchased from Invitrogen.

Storage and Final Concentration of Enzymes

We received PLD as a lyophilized powder and immediately dissolved it in a buffer solution containing 10 mM CsCl, 0.5 mM $CaCl_2$, and 10 mM cesium acetate with a pH of 5.5 (the same buffer was used for single channel recordings with this enzyme) to a final activity of 2,500 units mL^{-1}. We aliquoted and stored this PLD solution at −80° C until usage. According to Sigma Aldrich, one unit of PLD liberates 1.0 μmol of choline from L-α-phosphatidylcholine (egg yolk) per hour at pH 5.6 at 30 °C. The specific activity of this enzyme, provided by Sigma Aldrich, was more than 1670 units per milligram of protein. Assuming a pure enzyme and considering a molecular weight of ~92,000 Da,[28] a concentration of 1 unit mL^{-1} corresponds to a concentration of ~17.1 nM. We used this enzyme in a concentration range of ~15–40 nM in the bilayer chamber. For asymmetric bilayer experiments, we obtained inactivated PLD from a preparation that went through at least three freeze-thaw cycles, followed by extended storage at 4° C.

We received PI-PLC with an activity of 100 units mL^{-1} in a solution containing 20 mM Tris-HCl, pH 7.5, 1 mM EDTA, 0.01 % sodium azide, and 50% glycerol from Invitrogen, and stored it at −80° C. After thawing this enzyme preparation for the first time, we diluted it 10-fold in a buffer solution containing 20 mM KCl, 10 mM HEPES, pH 7.4 (this buffer was used for single channel recordings with this enzyme). We then aliquoted and stored the diluted enzyme solution at −80° C until usage. The unit definition for this enzyme, according to Invitrogen, is the amount of enzyme that converts 1 μmol of substrate to product per minute under the conditions of the assay. The specific activity of this enzyme, according to Invitrogen, was at least 1,000 units per milligram of protein. Assuming a pure enzyme and considering a molecular weight of ~35,000 Da, a concentration of 1 unit mL^{-1} corresponds to ~10.9 nM. We used this enzyme in a concentration range of ~43–86 pM in the bilayer setup. Therefore, with the standard bilayer setup used here, which had a volume of 3–4 mL, we were able to sense the activity of 172 femtomoles of PLC enzyme. It may be worth to point out that microfabricated bilayer setups[24,26] have the capacity of measuring single ion channel conductance in volumes as small as 10 μL. Employing such miniaturized setups for the assays developed here, may make it possible to quantify the activity of 430 attomoles of PLC.

To minimize loss of enzyme activity due to storage of these enzymes in solution, we always thawed fresh aliquots of enzyme solutions shortly before addition to the bilayer setup.

Formation of Planar Lipid Bilayers

We formed planar lipid bilayers[29] with the “folding technique”[11,30] in a custom-made bilayer setup fabricated in Teflon with two compartments of 3 or 4 mL capacity. We separated these

two compartments by a thin Teflon film that contained one aperture with a diameter of ~100 μm (Eastern Scientific Inc.). We used vacuum grease (Corning) to attach the Teflon film to the chamber and to create a water tight seal between the two compartments. To facilitate bilayer formation, we pretreated the area surrounding the aperture of the Teflon film on each side with 2 μL of 5% (v/v) hexadecane in pentane. After addition of 1 mL of appropriate electrolyte (see below) to each compartment, we spread 3–5 μL of a lipid solution in pentane (25 mg mL^{-1} for DiPhyPC or 5 mg mL^{-1} for mixtures containing 90 mol% DiphyPC and 10 mol% phosphatidylinositol) at the air-water interface of the electrolyte solution and raised the liquid level by adding another 2 or 3 mL (depending on the compartment size) of electrolyte. Raising the liquid level in these two compartments above the aperture in the Teflon film resulted in the formation of a lipid bilayer from apposition of two lipid monolayers as described originally by Montal and Mueller[31]. If raising the liquid level did not immediately result in formation a bilayer over the aperture, we lowered the liquid level in one or both compartments, followed by raising the electrolyte solution again. We repeated this cycle until we obtained a bilayer with a minimum capacitance of 70 pF.

The electrolyte solution for the experiments with PLD contained 10 mM CsCl, 0.5 mM $CaCl_2$, and 10 mM cesium acetate at a pH of 5.5 (adjusted with HCl). For experiments with PLC, the electrolyte contained 20 mM KCl and 10 mM HEPES at a pH of 7.4 (adjusted with KOH). We chose electrolytes with low ionic strength for these single channel recordings because the charge-induced local increase in cation concentration close to a membrane affects the gA conductance more significantly under conditions of low ionic strength compared to conditions of high ionic strength.[11,14]

Single Channel Recordings

Once a stable lipid bilayer was obtained, we gradually added small volumes (0.1 μL) of a solution of 10 ng mL^{-1} gA in isopropanol (Acros Organics) to both compartments of the bilayer setup until one to six gA channels were inserted in the bilayer at the same time. We chose isopropanol as solvent for gA since tertiary alcohols are not substrates for PLD as opposed to primary and secondary alcohols. After each addition of gA, we mixed the bilayer chambers by stirring the solutions in both compartments for at least 3 min (we confirmed previously that a small droplet of food dye was completely mixed in the setup within 2 min of stirring). In these experiments the final concentration of gA in the bilayer chamber was in the range of 0.1–2.0 pM. This range of gA concentration corresponds to 0.3–8 femtomoles of gA in the chamber with a volume of 3–4 mL; the total amount of lipid in each compartment was ~150 nanomoles, leading to a lipid to gA ratio of $\sim 10^8$. To measure the single channel conductance of gA pores, [23,32] we recorded current traces versus time while applying different voltages in the range of ±100 mV. We performed these single channel recordings in “voltage clamp mode” using Ag/AgCl pellet electrodes (Warner Instruments) in both compartments of the bilayer setup. Data acquisition and storage was carried out using a custom software written in Labview by Daniel J. Estes in combination with a Geneclamp 500 amplifier from Axon Instruments (set to a gain of 100 mV pA^{-1} and a filter cutoff frequency of 2 kHz). The data acquisition board (National Instruments) that was connected to the amplifier was set to a sampling frequency of 15 kHz. All recordings were carried out at a temperature of ~22° C.

We performed the analysis of the single channel current traces by computing histograms of the currents from the original current versus time traces with Clampfit 9.2 software (Axon Instruments). From these histograms, we extracted the mean current amplitude of gA channel opening and closing events. All conductance values were obtained from the slopes of current amplitudes versus voltage (I–V) curves (see the next section for more details on this analysis).

In order to reduce the noise in these single channel recordings, we mounted the bilayer setup on a low noise stir plate (Stir-2, Warner Instruments), which was placed on a bench top vibration

isolation platform (50 BM-4, Minus K Technology) inside a Faraday cage from Warner Instruments. In addition, we found that we reached the minimum noise level by placing the aforementioned setup on top of a second vibration isolation table (63–500 series from TMC) with a Faraday cage.

Cleaning of the Planar Lipid Bilayer Setup

In order to ensure recordings from high quality bilayers without contaminations from previous experiments, we cleaned the bilayer chamber and setup in the following way: We removed the Teflon film that was previously mounted by vacuum grease to separate two compartments of the bilayer setup, and we cleaned the film by several washes with a stream of chloroform from a Teflon squirt bottle, followed by air drying before storage. Second, we rinsed the chamber with deionized water, followed by ethanol, and finally by chloroform. After two chloroform rinses, we used a Kimwipe tissue to clean the inside walls of the chamber such that all the vacuum grease was removed, and we, again, rinsed the chamber with chloroform. We stored the chamber in chloroform between experiments. Note, all steps with solvents (in particular chloroform) were carried out in a chemical fume hood.

Supplementary Material

Refer to Web version on PubMed Central for supplementary material.

Acknowledgments

This work was supported by NIH (M.M., 1R01GM081705), a Barbour Scholarship (S.M.), the UCSD Academic Senate, a Hellman faculty fellowship for J.Y., and the UCSD Center for AIDS Research (NIAID 5 P30 AI36214).

References

1. Brown HA, Henage LG, Preininger AM, Xiang Y, Exton JH. Lipidomics and Bioactive Lipids 2007;434:49–87.
2. Huang P, Frohman MA. Expert Opin Ther Targets 2007;11:707–716. [PubMed: 17465727]Tappia PS, Dent MR, Dhalla NS. Free Radical Bio Med 2006;41:349–361. [PubMed: 16843818]
3. Scott SA, Selvy PE, Buck JR, Cho HP, Criswell TL, Thomas AL, Armstrong MD, Arteaga CL, Lindsley CW, Brown HA. Nat Chem Biol 2009;5:108–117. [PubMed: 19136975]
4. Deems RA, Eaton BR, Dennis EA. J Biol Chem 1975;250:9013–9020. [PubMed: 1194274]Jain MK, Berg OG. Biochim Biophys Acta 1989;1002:127–156. [PubMed: 2649150]
5. Volwerk JJ, Filthuth E, Griffith OH, Jain MK. Biochemistry 1994;33:3464–3474. [PubMed: 8142343]
6. Bayburt T, Yu BZ, Street I, Ghomashchi F, Laliberte F, Perrier H, Wang ZY, Homan R, Jain MK, Gelb MH. Anal Biochem 1995;232:7–23. [PubMed: 8600835]
7. Imamura S, Horiuti Y. J Biochem 1978;83:677–680. [PubMed: 641031]
8. Kuppe K, Kerth A, Blume A, Ulbrich-Hofmann R. Chembiochem 2008;9:2853–2859. [PubMed: 18942690]
9. Brake JM, Daschner MK, Luk YY, Abbott NL. Science 2003;302:2094–2097. [PubMed: 14684814] Hartono D, Bi XY, Yang KL, Yung LYL. Adv Funct Mater 2008;18:2938–2945.
10. Blake S, Mayer T, Mayer M, Yang J. Chembiochem 2006;7:433–435. [PubMed: 16444770]Danelon C, Lindemann M, Borin C, Fournier D, Winterhalter M. IEEE Trans NanoBiosci 2004;3:46–48.Mayer M, Semetey V, Gitlin I, Yang J, Whitesides GM. J Am Chem Soc 2008;130:1453–1465. [PubMed: 18179217]Schmidt C, Mayer M, Vogel H. Angew Chem Int Ed 2000;39:3137–3140.
11. Capone R, Blake S, Restrepo MR, Yang J, Mayer M. J Am Chem Soc 2007;129:9737–9745. [PubMed: 17625848]
12. Winiski AP, McLaughlin AC, McDaniel RV, Eisenberg M, McLaughlin S. Biochemistry 1986;25:8206–8214. [PubMed: 3814579]
13. Andersen OS, Koeppe RE, Roux B. IEEE Trans NanoBiosci 2005;4:10–20.

14. Apell HJ, Bamberg E, Lauger P. Biochim Biophys Acta 1979;552:369–378. [PubMed: 87221] Rostovtseva TK, Aguilella VM, Vodyanoy I, Bezrukov SM, Parsegian VA. Biophys J 1998;75:1783–1792. [PubMed: 9746520]
15. Griffith OH, Ryan M. BBA-Mol Cell Biol L 1999;1441:237–254.
16. Heinz DW, Essen LO, Williams RL. J Mol Biol 1998;275:635–650. [PubMed: 9466937]
17. These lipid bilayers were typically stable for 1–3 h.
18. We chose a hyperbolic function, because Hille described the increase in γ as a function of the bulk conc. of cations with a hyperbolic function. Here, the charge-induced local increase in cation conc. near a charged membrane has a similar effect as an increase of the cation conc. in the bulk solution. See Hille, B. Ion Channels of Excitable Membranes. Vol. 3. Sinauer Associates, Inc; Sunderland, Massachusetts, U.S.A: 2001.
19. Hovis and co-workers have also reported the formation of PA-rich domains in supported lipid bilayers (Giger K, Lamberson ER, Hovis JS. Langmuir 2009;25:71–74. [PubMed: 19067589]Cambrea LR, Haque F, Schieler JL, Rochet JC, Hovis JS. Biophys J 2007;93:1630–1638. [PubMed: 17483164]). Since domain formation could increase the permeability of ions through the bilayers, we used only the difference between two distinct, well defined current levels which was reached by an abrupt, stepwise change, to extract single channel conductances of individual gA pores. In this way, even a gradual increase in permeability through the bilayer (which may be caused by gradual domain formation) would not influence the quantification of the amplitude of single current steps.
20. Tou JS, Urbizo C. Cell Signal 2001;13:191–197. [PubMed: 11282457]
21. Madesh M, Balasubramanian KA. BBA-Lipid Lipid Met 1998;1389:206–212.
22. This simple model does not account for the heterogeneous nature of the catalytic reaction of PLD on a bilayer membrane. It also does not account for the possibility of product inhibition by PA lipids (Baszkin, A.; Norde, W., editors. physical chemistry of biological interfaces. Marcel Dekker Inc; New York: 2000.).
23. Kang XF, Cheley S, Rice-Ficht AC, Bayley H. J Am Chem Soc 2007;129:4701–4705. [PubMed: 17375923]Le Pioufle B, Suzuki H, Tabata KV, Noji H, Takeuchi S. Anal Chem 2008;80:328–332. [PubMed: 18001126]
24. Bruggemann A, Farre C, Haarmann C, Haythornthwaite A, Kreir M, Stoelzle S, George M, Fertig N. Methods Mol Biol 2008;491:165–76. [PubMed: 18998092]Kreir M, Farre C, Beckler M, George M, Fertig N. Lab on a Chip 2008;8:587–595. [PubMed: 18369514]Mach T, Chimerel C, Fritz J, Fertig N, Winterhalter M, Fuetterer C. Anal Bioanal Chem 2008;390:841–846. [PubMed: 17972068]
25. Mayer M, Kriebel JK, Tosteson MT, Whitesides GM. Biophys J 2003;85:2684–2695. [PubMed: 14507731]Peterman MC, Ziebarth JM, Braha O, Bayley H, Fishman HA, Bloom DM. Biomed Microdevices 2002;4:231–236.
26. Jeon TJ, Poulos JL, Schmidt JJ. Lab on a Chip 2008;8:1742–1744. [PubMed: 18813400]
27. Stankovic CJ, Delfino JM, Schreiber SL. Anal Biochem 1990;184:100–103. [PubMed: 1690956]
28. Younus H, Schops R, Lerchner A, Rucknagel KP, Schierhorn A, Saleemuddin M, Ulbrich-Hofmann R. J Protein Chem 2003;22:499–508. [PubMed: 14703982]
29. Suzuki H, Tabata KV, Noji H, Takeuchi S. Langmuir 2006;22:1937–1942. [PubMed: 16460131] Winterhalter M. Curr Opin Colloid Interface Sci 2000;5:250–255.
30. Blake S, Capone R, Mayer M, Yang J. Bioconjugate Chem 2008;19:1614–1624.
31. Montal M, Mueller P. Proc Natl Acad Sci U S A 1972;69:3561–3566. [PubMed: 4509315]
32. Gowen JA, Markham JC, Morrison SE, Cross TA, Busath DD, Mapes EJ, Schumaker MF. Biophys J 2002;83:880–898. [PubMed: 12124271]Kelkar DA, Chattopadhyay A. BBA-Biomembranes 2007;1768:2011–2025. [PubMed: 17572379]Wong D, Jeon TJ, Schmidt J. Nanotechnology 2006;17:3710–3717.

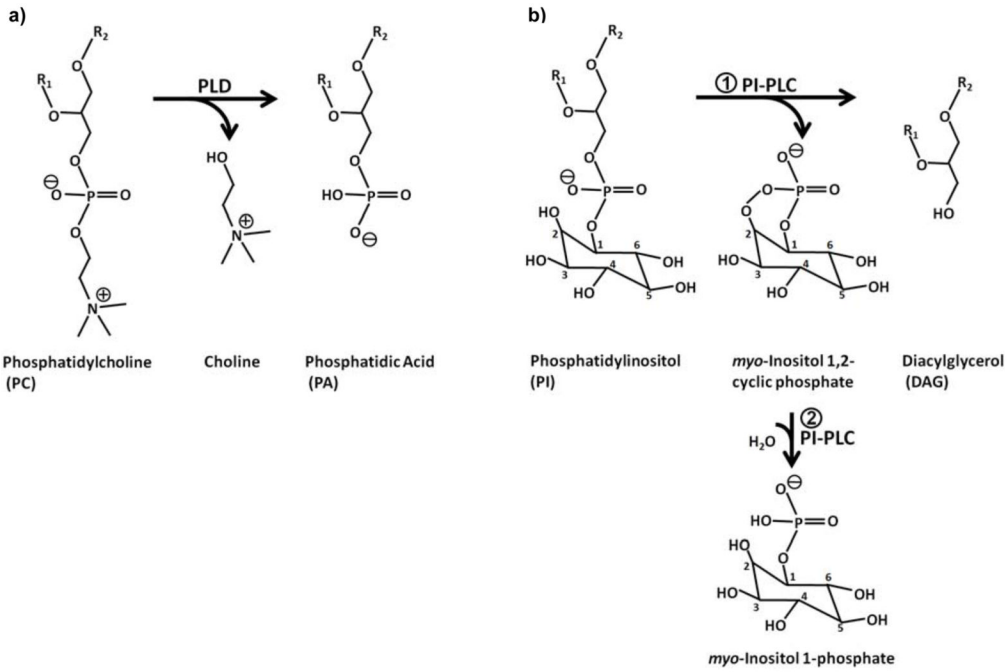

Figure 1.

Hydrolysis of phospholipids by phospholipases D or C (PLD and PLC). (a) PLD catalyzes the hydrolysis of electrically neutral (zwitterionic) phosphatidylcholine (PC) lipids to produce choline and negatively-charged phosphatidic acid (PA) lipids.[1] (b) Phosphatidylinositol-specific PLC (PI-PLC) catalyzes the hydrolysis of PI lipids in two steps. In the first reaction, PI-PLC catalyzes hydrolysis of PI to produce electrically neutral diacylglycerol (DAG) lipids and soluble *myo*-inositol 1,2-cyclic phosphate and in the second, slower reaction PI-PLC hydrolyzes *myo*-inositol 1,2-cyclic phosphate to *myo*-inositol 1-phosphate.[15,16] R_1 and R_2 stand for any acyl chain of lipids.

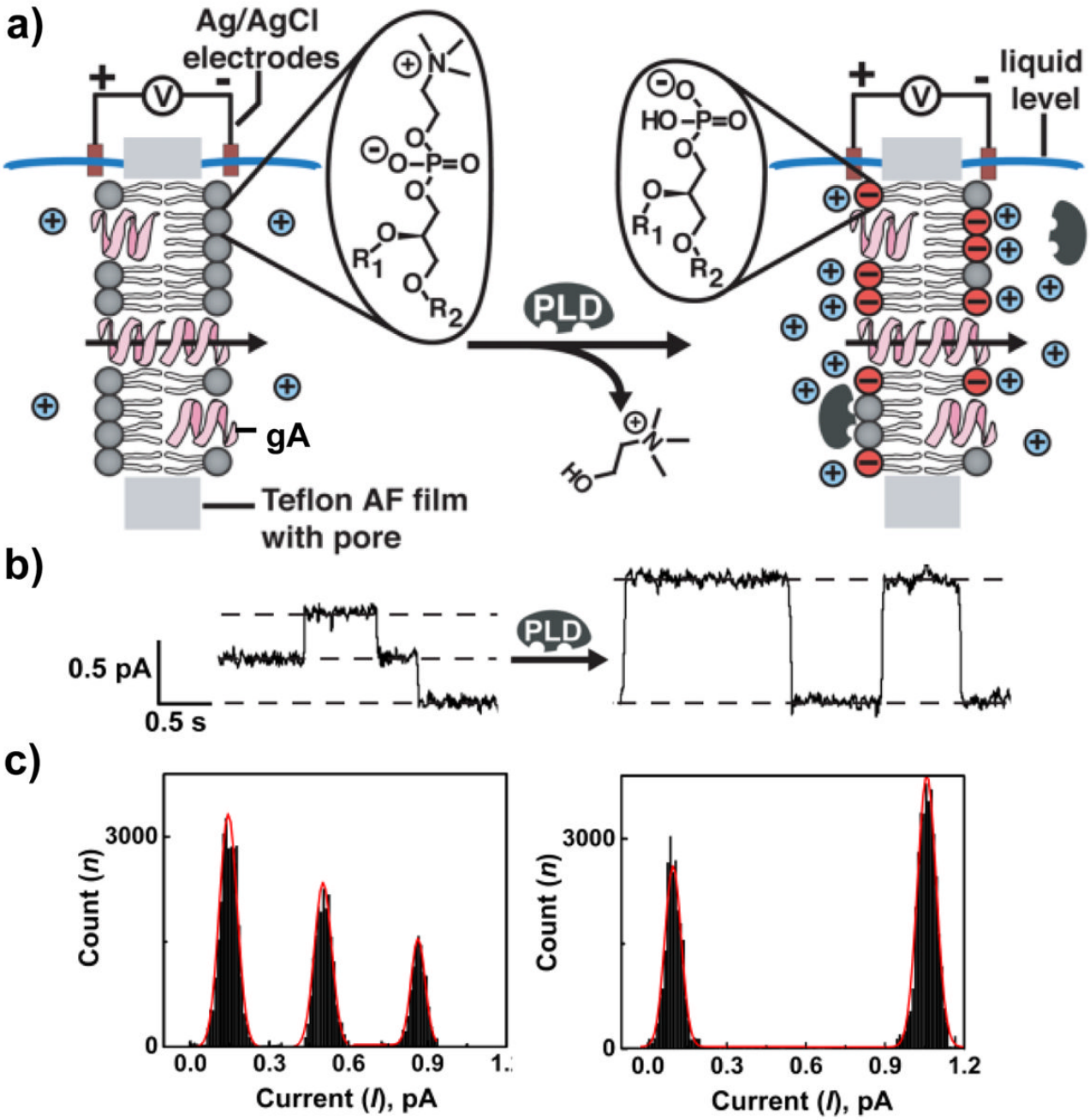

Figure 2.

Basic concept of monitoring the activity of PLD, *in situ*, on planar lipid bilayers by changes in single channel conductance of gA pores, γ. (a) As PLD hydrolyzes electrically neutral PC lipids and produces negatively-charged PA lipids, accumulation of cations close to the membrane surface leads to a significant increase in γ.[11,14] Negative charges are shown in red and positive ions are shown in blue. (b) Original current versus time recordings in the presence of 2 pM gA before and after addition of PLD; these current traces illustrate the increase in single channel current upon addition of PLD. (c) Corresponding histograms representing the PLD-induced shift in current distribution.

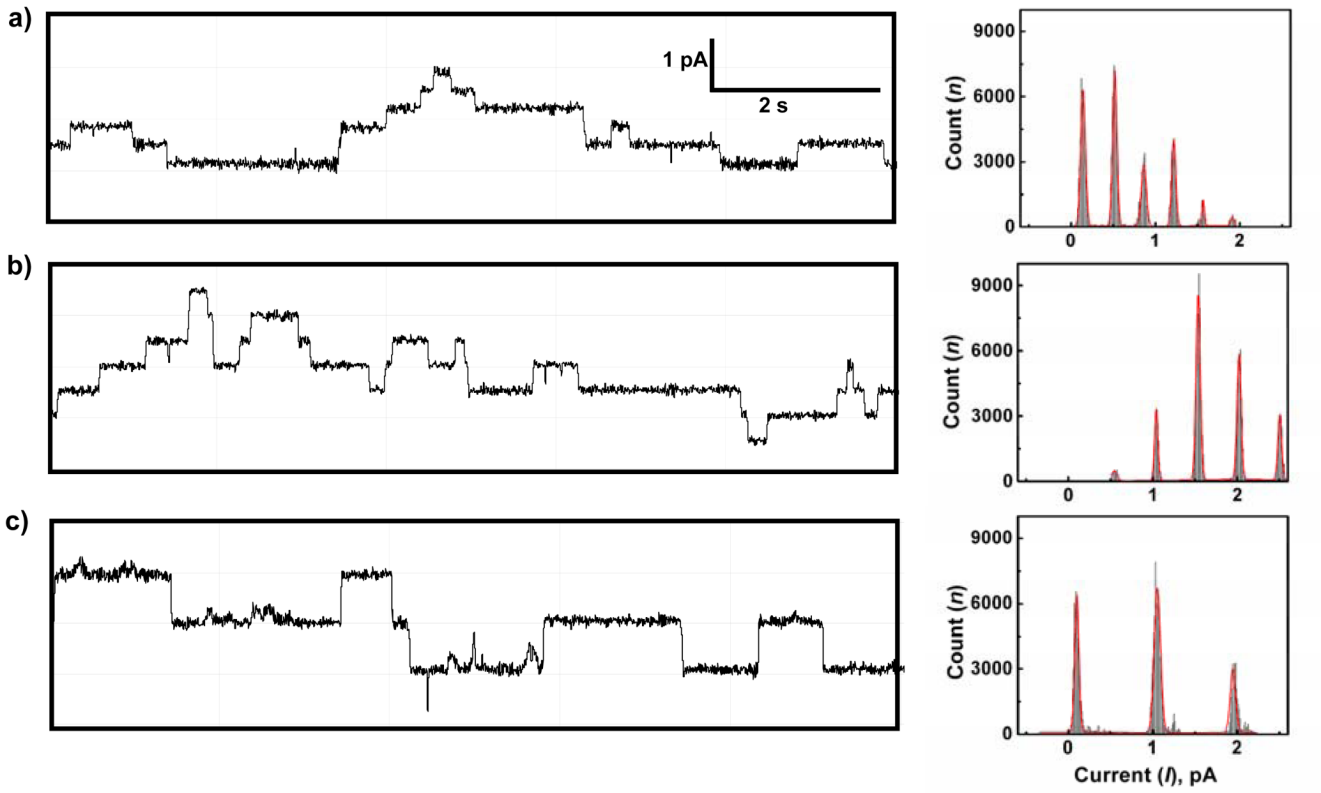

Figure 3.

Current versus time recordings in a lipid bilayer that contained gA channels (a) before addition of PLD and (b) 5 min, and (c) 13 min after addition of PLD (with a final concentration of 3.1 units·mL^{-1}). The applied voltage was +100 mV in all three recordings. Each step increase in current represents the formation of one gA channel and each step decrease represents the dissociation of one gA channel. The corresponding all point histograms on the right illustrate the distribution of the recorded current in each trace (so called current histograms). The difference in current between adjacent peaks in these current histograms reflects the current amplitude of step-wise gA events. These histograms, therefore, demonstrate a time-dependent increase in current amplitude of gA events.

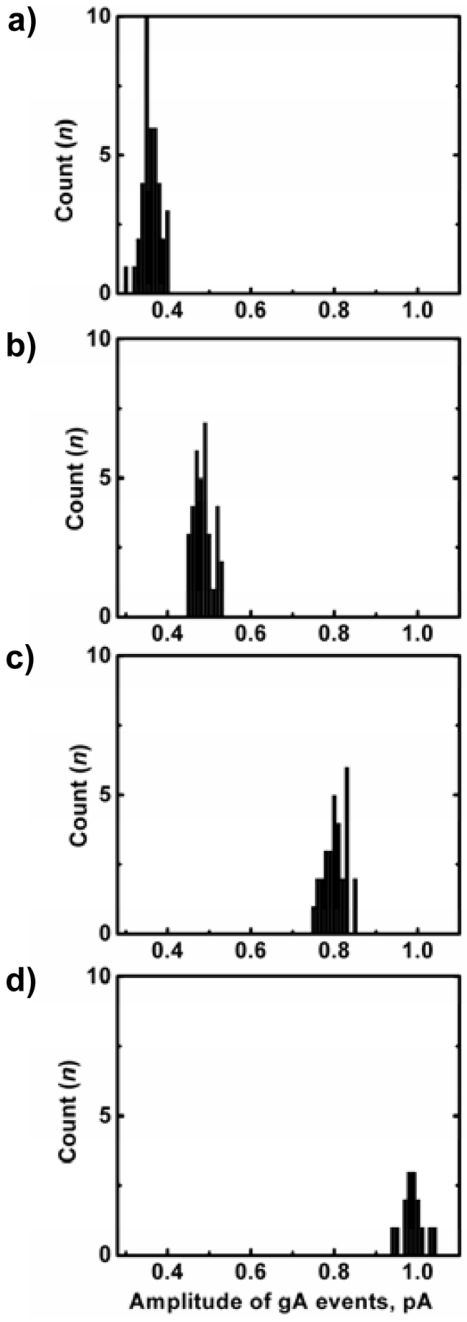

Figure 4.

Distribution of current amplitudes of individual gA opening and closing events (so called event histograms) at differnt time points after addition of 3.1 units·mL^{-1} PLD to a PC bilayer. Event histograms of current amplitudes of events (a) before addition of PLD, (b) 5 min, (c) 7 min, and (d) 13 min after addition of PLD. Ion channel recordings proceeded at an applied potential of +100 mV in an electrolyte solution containing 10 mM CsCl, 0.5 mM $CaCl_2$, and 10 mM cesium acetate at pH 5.5.

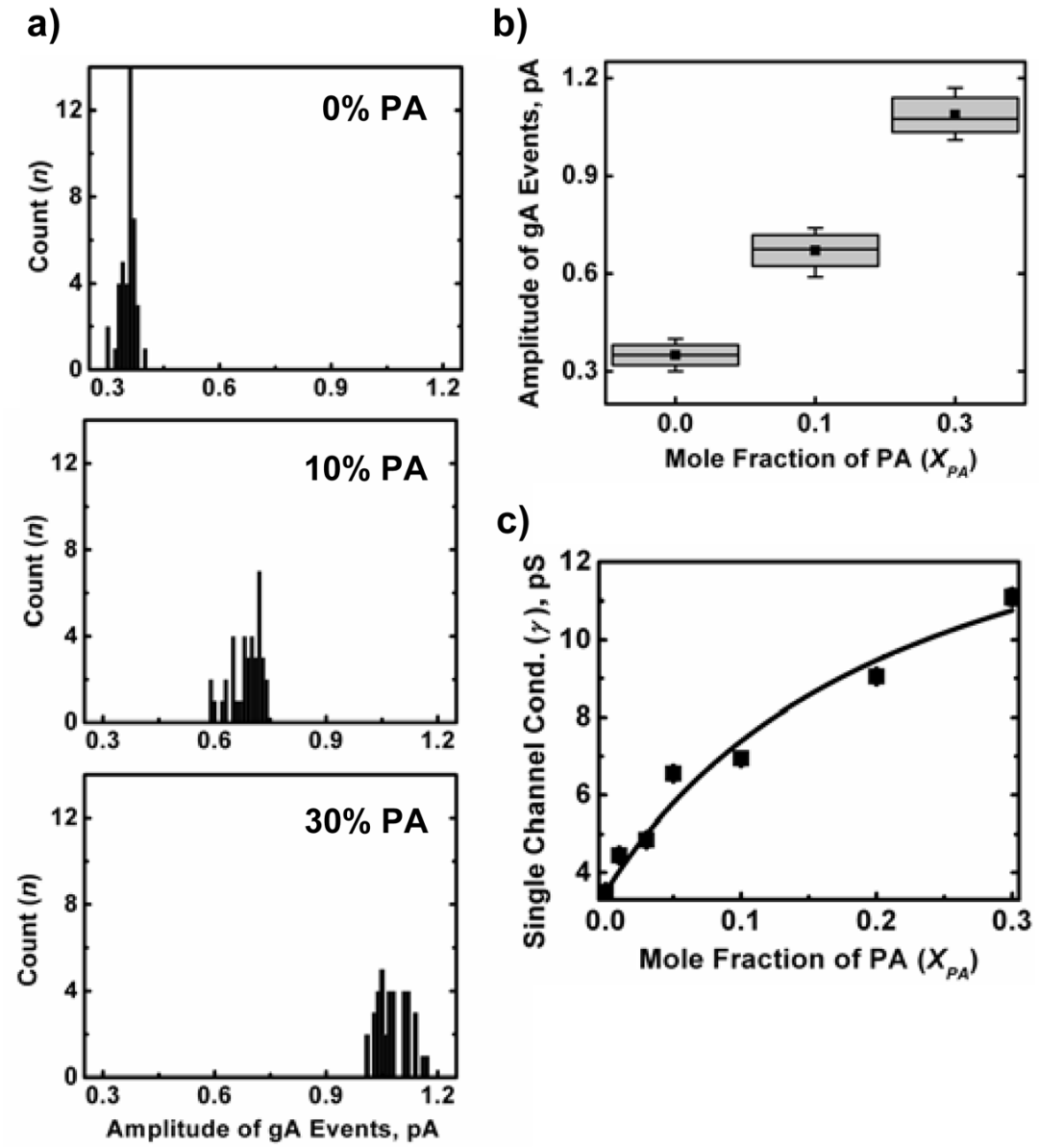

Figure 5.

Distribution of current amplitudes of gA events in electrically neutral PC bilayers with different contents of negatively-charged PA lipids and the coressponding calibration curve of γ as a function of PA content of the bilayer. (a) Event histograms of current amplitudes of gA events in PC bilayers that contained 0, 10, and 30 mol% PA lipids. (b) Box chart showing the distribution of current amplitudes of gA events in these bilayers. The black squares represent the mean current amplitude of gA events. The boxes represent the standard deviation of the mean amplitude. The horizontal line in the boxes represents the median of the distribution and the error bars represent the minimum and maximum current amplitudes. (c) Calibration curve of γ versus the mole fraction of negatively-charged PA lipids, X_{PA}, in PC membranes. The graph shows the best fit ($R2 = 0.97$, $N = 7$) to a hyperbolic function[18] of the form $\gamma = \gamma_0 + (A \times X_{PA})/(B + X_{PA})$, where A (pS) and B (unitless) are fitting parameters, and γ_0 (pS) is γ before the addition of PLD. Ion channel recordings proceeded at an applied potential of +100 mV in

an electrolyte solution containg 10 mM CsCl, 0.5 mM $CaCl_2$, and 10 mM cesium acetate at pH 5.5.

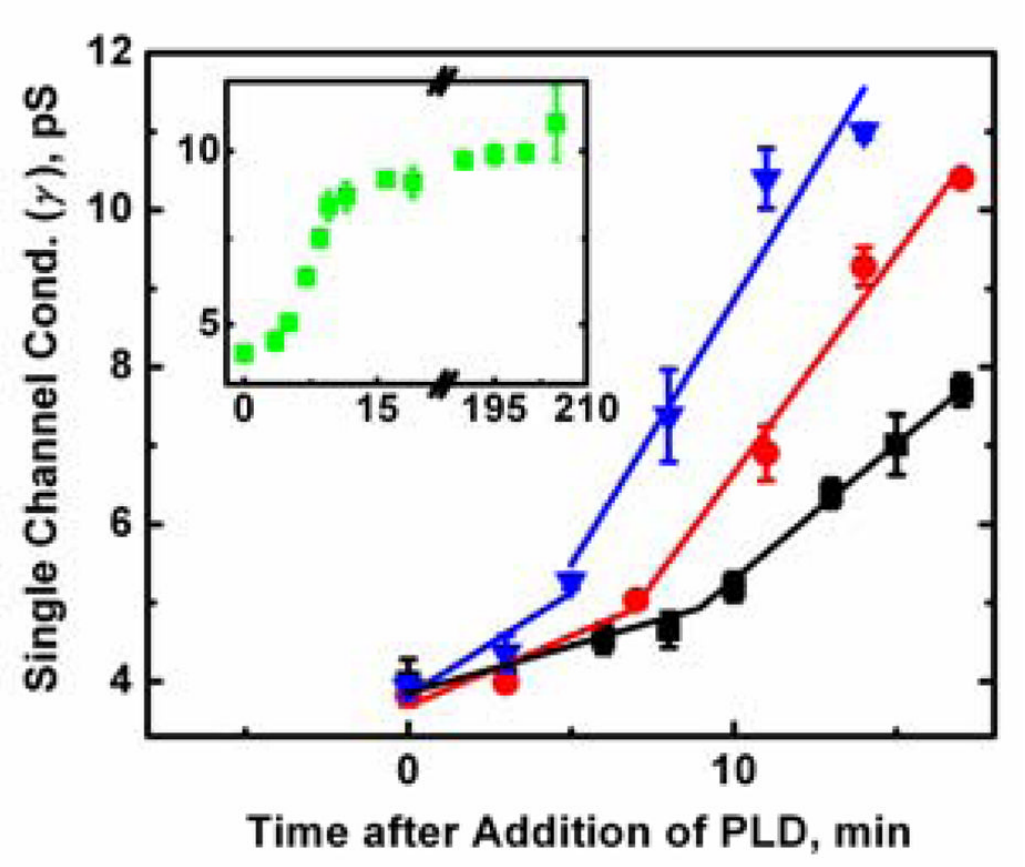

Figure 6.

Single channel conductance of gA pores, γ, as a function of time after addition of PLD. Time-dependent increase in γ upon addition of various conc. of PLD, including: (■) 2.3, (●) 3.1, and (▼;) 5.2 units·mL^{-1} corresponding to PLD conc. of ~15–40 nM to a pure PC bilayer. The lines represent the best linear fits. For each PLD concentration, points within the lag phase and after the lag phase were fitted separately. Typically the slope after the lag phase was ~3-fold larger than the slope during the lag phase (see Supporting Information for more details). The inset shows the enzymatic hydrolysis by 4.2 units·mL^{-1} of PLD over an extended period of time. Error bars represent the standard error of the mean ($N \geq 3$). Ion channel recordings proceeded at an applied voltage of +100 mV in an aqueous electrolyte containing 10 mM CsCl, 0.5 mM $CaCl_2$, and 10 mM cesium acetate at pH 5.5.

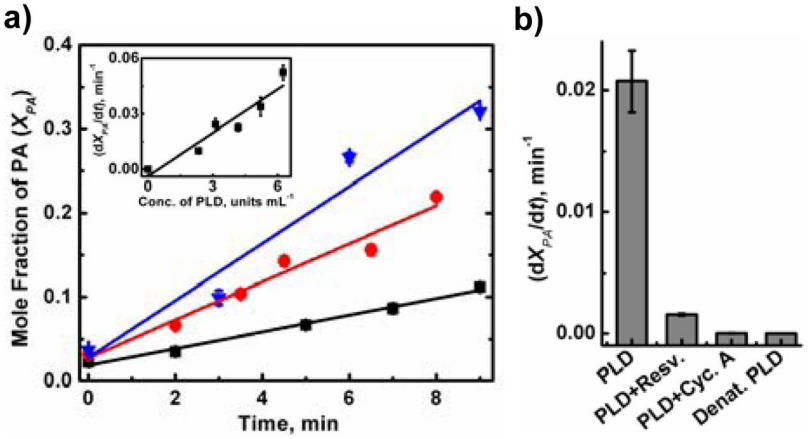

Figure 7.

PA membrane content, X_{PA}, as a function of time and the initial velocity (dX_{PA}/dt) of PC hydrolysis as a function of PLD concentration and in the presence of PLD inhibitors. (a) Time-dependent change in X_{PA} in PC membranes after addition of (■) 2.3, (●) 4.2, and (▼;) 5.2 units·mL^{-1} PLD. The *x*-axis shows the time after the lag phase. The lines represent the best linear fits to the data. The inset depicts the slope from these linear fits, representing dX_{PA}/dt as a function of PLD concentration. (b) Comparison of the initial velocity (dX_{PA}/dt) of PC hydrolysis by 4.2 units·mL⁻1 of PLD in the presence of two inhibitors, resveratrol (final conc. ~130 μM) and cyclosporin A (final conc. 5 μM), and after adding heat-denatured PLD. All error bars show the error of the linear fits used to obtain dX_{PA}/dt.

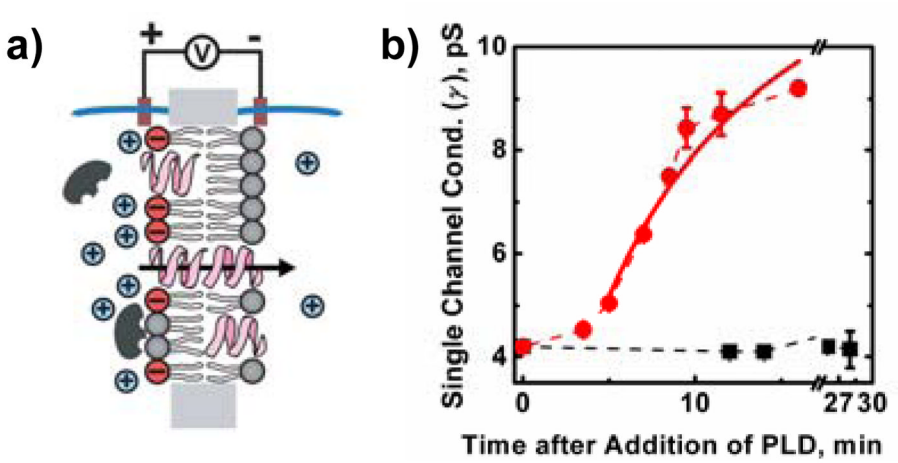

Figure 8.

Generation of planar lipid bilayers with transverse lipid asymmetry by addition of active PLD to one compartment of the bilayer setup and addition of inactive PLD to the other compartment. (a) Schematic representation of PLD-induced lipid asymmetry in a bilayer. (b) Graph showing changes in γ when the polarity was such that (●) the entrance of gA pores was located in the compartment with 4.2 units·mL^{-1} active PLD, or (■) in the compartment with 4.2 units·mL^{-1} inactive PLD. Error bars represent the standard error of the mean ($N \geq 3$). The solid red curve illustrates the best fit ($R^2 = 0.93$, $N = 6$) of the points shown in red to Eq. 3. For this fit only data after the lag phase were included (the point at ~5 min corresponds to X_{PA} ~0.03 and marks the end of lag phase).

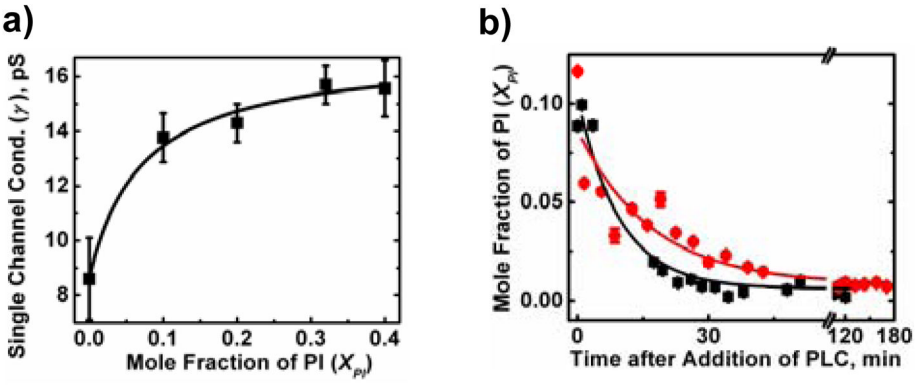

Figure 9.

Calibration curve of single channel conductance of gA, γ, as a function of PI membrane content and time-dependent changes in PI membrane content upon PLC addition. (a) Calibration curve of γ as a function of the mole fraction of PI (X_{PI}) in PC membranes. The black curve corresponds to Eq. 4 and represents the best fit ($R^2 = 0.93$, $N = 5$) to a hyperbolic function. (b) Decrease in X_{PI} of membranes after addition of (●) 0.0015 and (■) 0.0030 units·mL^{-1} PLC. The solid curves show the best fit of the data to an exponential decay of the form $X_{PI} = X_{PI,0} \times \exp(-k \times t)$, where $X_{PI,0} = 0.1$, while k (min^{-1}) is the fitting parameter at a given enzyme concentration, and t (min) is time. All error bars represent the standard error of the mean ($N \geq 3$). Single channel recordings proceeded at an applied voltage of +100 mV in an electrolyte containing 20 mM KCl and 10 mM HEPES at pH 7.4.